Journal of Superconductivity and Novel Magnetism (2020) 33:3321–3331
https://doi.org/10.1007/s10948-020-05599-8

ORIGINAL PAPER

Structural and Magneto-Electrical Properties of $Bi_{2-x}Sm_xSr_2CaCu_2O_{8+\delta}$ High T_c Superconductor Prepared by Pechini Method

Mourad Mimouni[1] · Mohammed Sadok Mahboub[1] · Nabil Mahamdioua[2] · Mohamed Fayçal Mosbah[3] · Ghani Rihia[1] · Soria Zeroual[1] · Mebrouk Ghougali[1] · Sevgui Polat Altintas[4] · Akram Alhussein[5]

Received: 28 May 2020 / Accepted: 9 July 2020 / Published online: 15 July 2020

Abstract
Polycrystalline superconducting samples of $Bi_{2-x}Sm_xSr_2CaCu_2O_{8+\delta}$ were synthesized using Pechini method with different doping Sm concentrations ($x = 0.0$, 0.05, and 0.10) and investigated. FTIR spectroscopy showed that our final samples are totally free of organic elements. Le Bail refinement revealed that they were crystallized in the Bi-2212 phase. A small amount of the omnipresent Bi-2201 phase appeared as an impurity phase in all samples, whereas a small amount of Bi-2223 appeared only in the case of $x = 0.5$. In one hand, the Sm doping decreases the cell parameters, and in other hand, it leads to a transformation into a pseudo-tetragonal structure in the case of $x = 0.10$.The modulation was found to be incommensurate and increases with Sm content. The magneto-electrical resistivity curves show a transition to the superconductor state. The critical temperature T_C decreases with the Sm doping, whereas the activation energy U_0 increased from 53.4 meV to 68.9 meV.

Keywords High T_c superconductors · Samarium doping · Magneto-resistivity · Pechini method

1 Introduction

$Bi_2Sr_2Ca_{n-1}Cu_nO_{2n+4+\delta}$ compounds ($n = 1$; Bi-2201, $n = 2$; Bi-2212, $n = 3$; Bi-2223), known as BSCCO systems, were discovered by Maeda et al. [1]. Their physical properties were investigated and showed great scientific interests in many domains like high power, high field magnet, and current limiter applications [2, 3]. The $Bi_2Sr_2CaCu_2O_{8+d}$ system, known as the Bi-2212, has a high critical temperature [4] and a good chemical stability [5]. The $Bi_2Sr_2CaCu_2O_{8+\delta}$ system known as the Bi-2212 phase can be prepared by different techniques; among them, the Pechini method [6] was used in the present work.

Several studies reported the influence of the doping by rare earth elements in the cationic site of Bi-2212 phase [7–10]. In the doped Bi-2212 phase, some changes appear in structures and physical properties [11]. When Sr is substituted by Gd or Eu in the Bi-2212 phase, both the critical temperature (T_C) and the critical current density (J_C) increased [12, 13]. Addition of dysprosium in the Bi-2212 phase causes significant changes in the lattice parameters, microstructure, holes concentration, normal state resistivity, and flux pinning strength of the system [14]. The substitution of calcium by yttrium in the Bi-2212 phase affects the cell parameters and surface morphology. The critical temperature T_C increases by increasing the yttrium content up to 0.30, and decreases with further increase of Y. A similar behavior was obtained for the absolute values of true hardness Ht [15]. However, the substitution of Bi by Ni in a similar system (Bi-2212 phase) does not lead to any changes in the transition temperature (T_C) [16]. A.T. Ulgen et al. found that the substitution of bismuth by thulium in the same phase improved regularly the characteristic features by the increment in the Tm impurity level up to $x = 0.07$. Beyond this value, the properties degraded dramatically [17]. Doping

✉ Mourad Mimouni
mimouni-mourad@univ-eloued.dz

[1] LEVRES Laboratory, University of El Oued, 39000 El Oued, Algeria

[2] LEND Laboratory, Mohammed Seddik Ben Yahia University, 18000 Jijel, Algeria

[3] University of Constantine1, 25000 Constantine, Algeria

[4] Physics Department, Faculty of Arts and Sciences, Bolu Abant İzzet Baysal University, Bolu, Turkey

[5] ICD-LASMIS, University of Technology of Troyes, 26 rue Lavoisier, 52800 Nogent, France

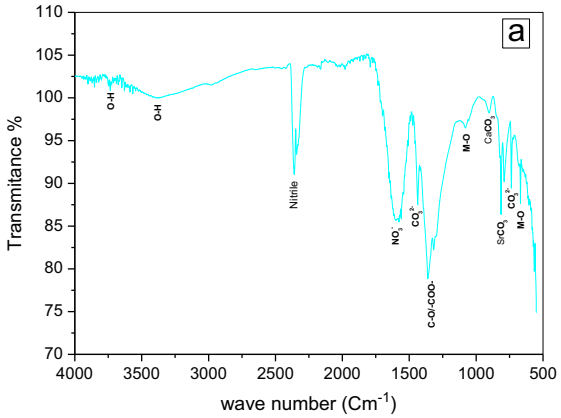
a
Transmitance %
wave number (Cm-1)
O-H
O-H
Nitrile
M-O
M-O

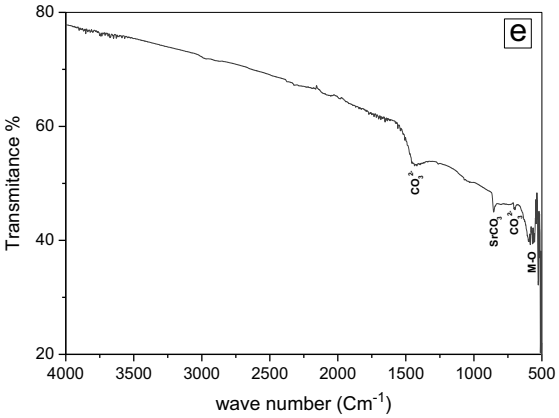
e
Transmitance %
wave number (Cm-1)
M-O

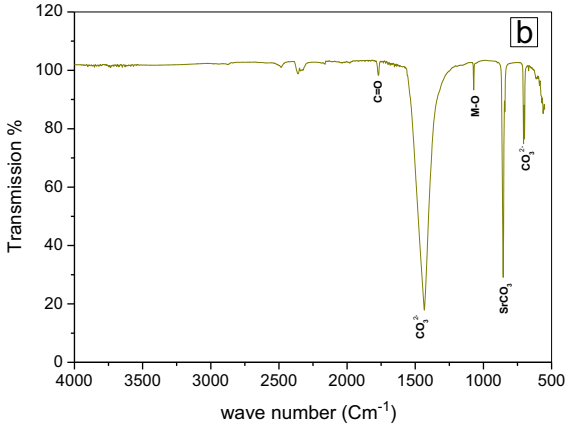
b
Transmission %
wave number (Cm-1)
C=O
M-O

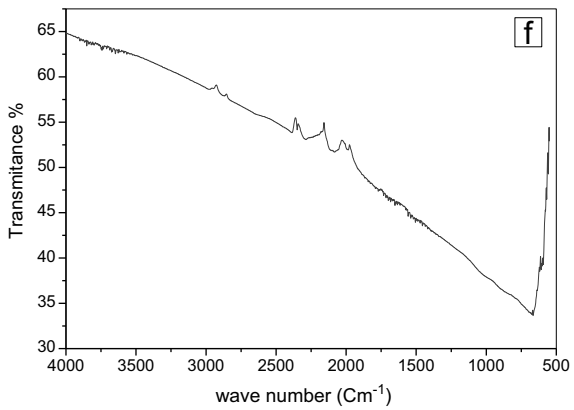
f
Transmitance %
wave number (Cm-1)

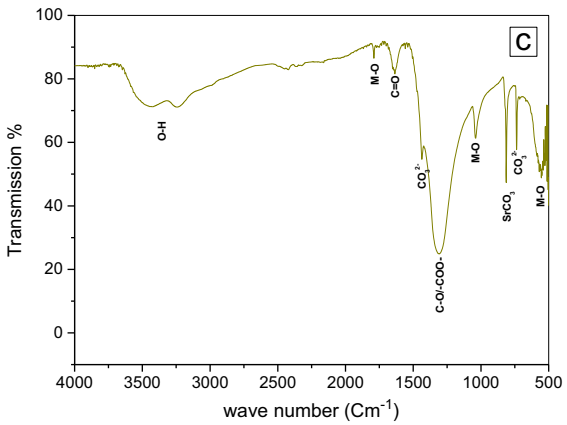
c
Transmission %
wave number (Cm-1)
O-H
M-O
C=O
M-O
M-O

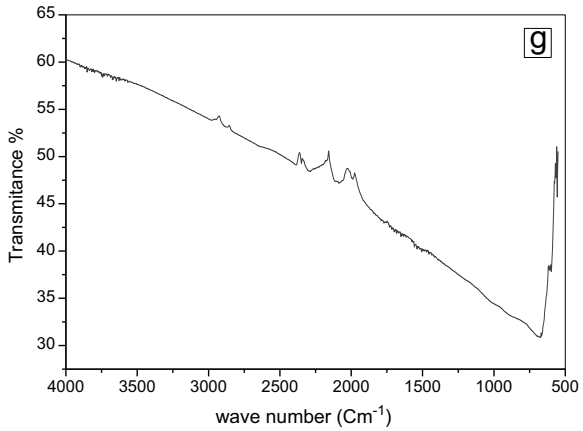
g
Transmitance %
wave number (Cm-1)

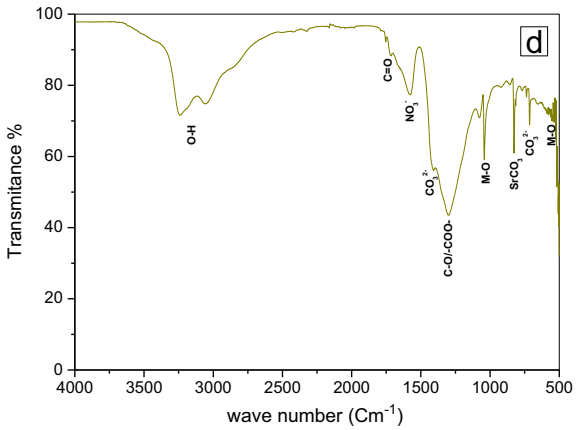
d
Transmitance %
wave number (Cm-1)
O-H
C=O
M-O
M-O

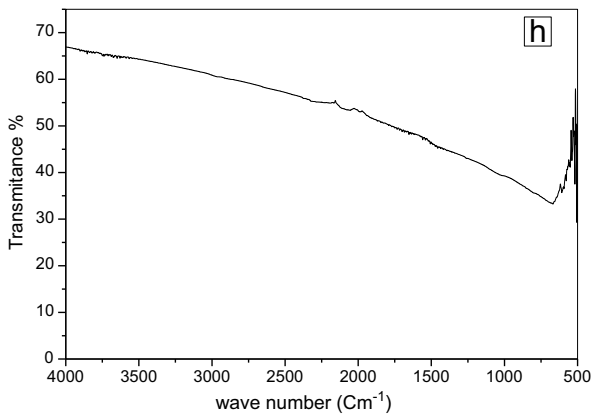
h
Transmitance %
wave number (Cm-1)

◀ **Fig. 1** FTIR spectrum of (**a**) Gel, (**b**) Sm00 (after combustion), (**c**) Sm05 (after combustion), (**d**) Sm10 (after combustion), (**e**) Sm00 (after calcination), (**f**) Sm05 (after calcination), (**g**) Sm10 (after calcination), and (**h**) Sm00 (after sintering)

with samarium substantially affects the superconducting and structural properties of BSCCO materials [18]. Low concentration doping of Ca by Sm decreases the c cell constant and increases the transition temperature value [19]. Kishore et al. [20] found that the quantity of the Bi-2212 phase increases and the critical temperature decreases as the samarium concentration increases. In another study, I. Hamadneh et al. [21] reported that replacing of strontium by samarium in the Bi(Pb)-2212 phase decreased the volume percentage of the 2223 phase and increased the lattice density. The addition of Sm in the Bi(Pb)-2212 phase enhances the superconductivity transition temperature T_C [22]. For the substitution of Bi by Sm, H. S. Kim et al. [23] reported that it facilitated the formation of the Bi-2223 phase in the Bi-1111 system, which increases the critical temperature. Until now, no work has investigated the effect of bismuth substitution by samarium in the Bi-2212 compounds.

In this work, a series of samples with the nominal composition of $Bi_{2-x}Sm_xSr_2CaCu_2O_{8+\delta}$ ($x = 0$, 0.05, and 0.10) were prepared by the Pechini method. This study focused on the effect of samarium doping in their Bi site, on the structure and its modulation, the microstructure, the electrical, and the magneto-electrical properties of these compounds.

2 Experimental

Analytical reagents Bi_2O_3 (99.5%), $SrCO_3$ (99%), Sm_2O_3 (99.9%), $CaCO_3$ (> 98.5%), and CuO (> 98%) were used as reactants in a molar ratio of Bi:Sm:Sr:Ca:Cu = 2-x: x: 2: 1: 2 where $x = 0$, 0.05, and 0.10. A little amount of nitric acid HNO_3 was used to dissolve oxides during 24 h at 70 °C in a magnetic agitator. The citric acid $C_6H_8O_7$ was used then as an organic fuel with a proportion of $n_{AC}/n_S = 1.5$, where n_{AC} and n_S are appropriate molar quantities of the citric acid and the sample, respectively. One ml of ethylene glycol as a polymerizing agent was added to the solution to terminate the dissolution and prepare a chelate which was transformed into a polymer with a homogeneous distribution of cations. We used ammonia solution (28%) in order to stabilize the pH value between 6 and 7; then, the mixture was gradually heated up to 130 °C (10 °C/min). After 1 h, a green-bluish gel was obtained through stirring and heating with the clearance of NO_x brown gas. In the aim to transform the gel into powder by self-combustion, the mixture was heated to 350 °C, and hence, a dark-brown precursor powder was gotten. The prepared precursor powders were manually ground in an agate mortar for 1 h and then calcined at 800 °C for 12 h with 5 °C/min in a muffle furnace. This gives an intermediate black powder. Such treatment allows the degradation of organic compounds. The calcined powder was ground and pelletized under 3 tons in a cylindrical die of 13-mm diameter. The pellets were then sintered at 830 °C for 20 h, then grounded again and re-pelletized for a second sintering at the same temperature for 30 h. In order to follow the disappearance and the formation of organic and inorganic bonds after each step of preparation, we used a FTIR Thermo Fisher Nicolet iS5 spectrometer. The structural analysis of samples was carried out by X-ray diffraction using a Proto AXRD Benchtop Powder X-ray diffractometer. The X-ray diffractograms were recorded with a step of 0.02°/s using CuK_α radiation. The refinement of the cell parameters and modulation vector was performed using Jana2006 program [24]. The microstructure was observed by a Tescan Vega3 scanning electron microscope (SEM). The resistivity measurements were carried out using the four-probe technique in the temperature range 4 K–300 K under zero and 0.7 T as an external magnetic field using a He-gas contact cryocooler and superconducting coil magnet from CRY industries. Hereafter, we label the samples Sm00, Sm05, and Sm10 to designate the samples with 0.0, 0.05, and 0.10 samarium content, respectively.

Table 1 Absorption bands in the FTIR results after each step of preparation

Band		M-O	CO_3^{2-}	$SrCO_3$	$CaCO_3$	C-O-COO-	NO_3^-	C=O	C ≡ N	O-H
Gel		6,671,077	7,331,442	808	902	1360	1590	–	2360	3300 3730
Combustion	Sm00	1077	7,021,436	852	–	–	–	1770	–	–
	Sm05	5,581,041 1794	7,331,430	815	–	1310	–	1640	–	3370
	Sm10	5,521,040	7,151,420	820	–	1300	1590	1718	–	3230
Calcination	Sm00	560	7,021,442	852	–	–	–	–	–	–
	Sm05	610	–	–	–	–	–	–	–	–
	Sm10	560	–	–	–	–	–	–	–	–
Sintering		530	–	–	–	–	–	–	–	–

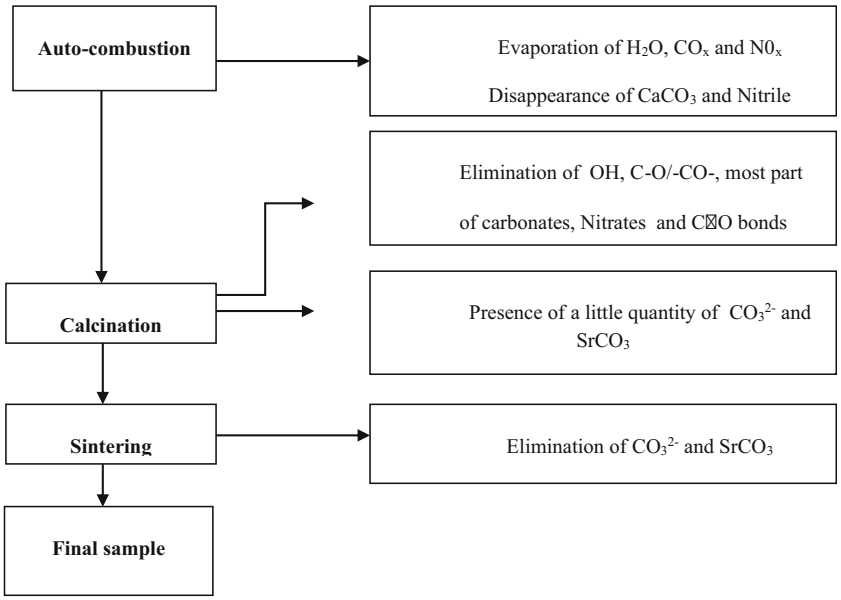

Fig. 2 Elimination of organic compounds from the undoped sample prepared by Pechini method

3 Results and Discussion

FTIR spectra of the gel, combustions, and precursors that were calcined at 800 °C and sintered at 830 °C are shown in Fig. 1. In the gel precursor of undoped sample, as an example (Fig. 1a), the presence of the peak at around 1600 cm^{-1}shows the complex formation in the BSCCO material [25]. Two bands due to the stretching vibration of the CO_3^{2-} appeared at 733 and 1442 cm^{-1}.Other peaks appeared and can be attributed to $SrCO_3$ at 808 cm^{-1}, $CaCO_3$ at 902 cm^{-1}, and metal oxide bands (M-O) at 665 and 1077 cm^{-1} [25]. Only a small peak corresponding to NO_3^- ions was found at 1590 cm^{-1}, which may indicate that most of its amount was consumed to produce gel [26]. The presence of O-H bands at 3300 $cm^{-1}$and 3730 cm^{-1} indicates the gel humidity. The peak attributed to nitrile band (C ≡ N) at 2360 cm^{-1} indicates the formation of amid resulting from the reaction between carboxylic acid and ammonia [27]. In addition, we notice the

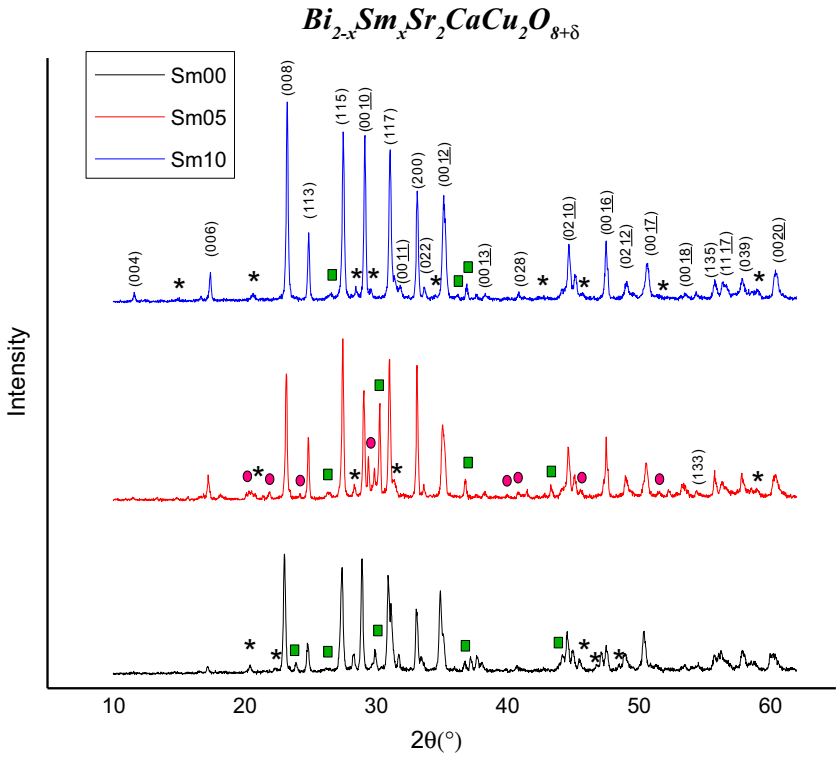

Fig. 3 X-ray diffraction pattern of Sm00, Sm05, and Sm10 with (■) Bi-2201, (●) Bi-2223, and (*) satellite peaks

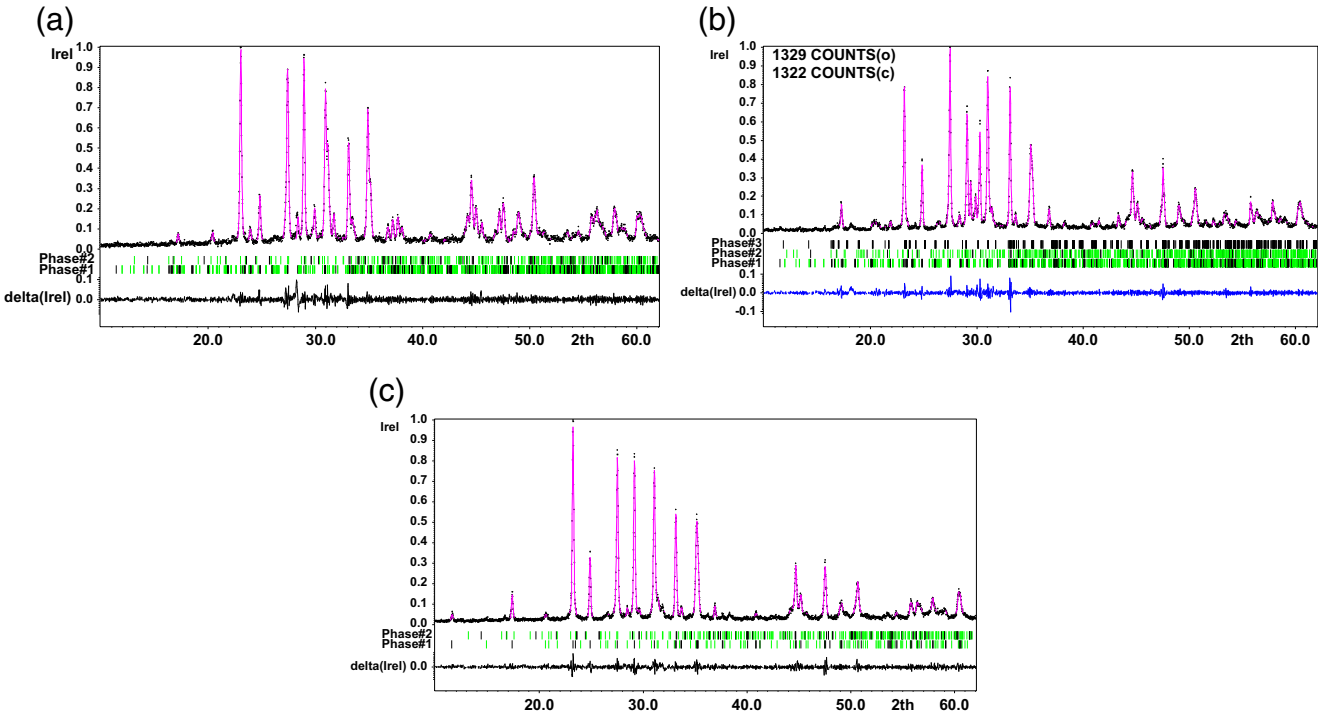

Fig. 4 Le Bail refinement result of (**a**) Sm00, (**b**) Sm05, and (**c**) Sm10 samples phase#1 (Bi-2212), phase#2 (Bi-2201), and phase#3 (Bi-2223).

decrease of the NO_3^- peak after the self-combustion. This signifies that the NO_x gas has evaporated during this step [28]. Furthermore, after calcinations, $CaCO_3$ was eliminated in all samples, while $SrCO_3$ persisted in the undoped one. It is also noticed that only the undoped sample contains bands corresponding to organic elements. Thus, we think that Sm may cause the disappearance of organic elements from the doped samples. Figure 1 h shows that after sintering there is no evidence of carbonates or any other impurities in the oxide powder.

We summarized in Table 1 the entire FTIR results after each preparation step of all our samples. In Fig. 2, we show the formation steps of the undoped sample elaborated by the Pechini method.

Figures 3 and 4 present the X-ray diffraction patterns and the Le Bail refinement profile of our samples respectively. They showed that they are well crystallized. The patterns

Table 2 Bi-2212 (%), F_{00l} (%), lattice parameters (a, b, c, v, and q), goodness of fit (GOF), and agreement factors (Rp,Rp,w) of Sm00, Sm05, and Sm10 samples

sample	Sm00	Sm05	Sm10
Bi-2212(%)	92.3	82	97
F_{00l}(%)	38.6	25	44.9
a(Å)	5.4244(4)	5.4128(4)	5.4062(3)
b(Å)	5.3874(4)	5.3976(3)	5.4068(3)
c(Å)	30.8136(20)	30.6790(19)	30.6338(17)
q/a*	0.2110(1)	0.2156(1)	0.2162(1)
V(Å^3)	900.4785	896.3216	895.4333
GOF	1.02	1.05	1.07
Rwp	10.88	10.67	10.38
Rp	7.64	7.74	7.34

Table 3 The satellite peaks position and indexation from Le Bail refinement of $Bi_{2-x}Sm_xSr_2CaCu_2O_{8+\delta}$ samples

Sample	2θ(°)	(h k l m)
Sm00	20.4	(0 0 8 $\bar{1}$)
	22.4	(0 1 6 $\bar{1}$)
	45.5	(−2 0 $\underline{10\bar{1}}$)
	46.8	(3 0 2 $\bar{1}$)
	48.5	(2 2 7 $\bar{1}$)
Sm05	20.4	(0 0 8 $\bar{1}$)
	28.3	(1 0 6 1)
	31.4	(1 1 9 $\bar{1}$)
	58.9	(1 3 5 1)
Sm10	15.0	(0 0 6 $\bar{1}$)
	20.4	(0 0 8 $\bar{1}$)
	28.5	(−1 1 5 $\bar{1}$)
	29.6	(2 0 2 $\bar{1}$)
	34.5	(0 2 4 $\bar{1}$)
	42.7	(0 2 $\underline{10\bar{1}}$)
	45.5	(−2 0 $\underline{10\bar{1}}$)
	51.5	(3 1 5 $\bar{1}$)
	58.9	(1 3 5 1)

Table 4 Estimated crystallite size of $Bi_{2-x}Sm_xSr_2CaCu_2O_{8+\delta}$ samples

Sample	Sm00	Sm05	Sm10
Crystallite size (nm)	9.2	11.4	9.8

revealed also that they are crystallized in the Bi-2212 phase. However, some small peaks corresponding to the Bi-2201 phase appears in all the samples, and over, that the Bi-2223 phase appears in the Sm05 sample. We note here that it is too difficult to avoid these two phases in such compounds [29].We note also that there are no other extra peaks, which means that the Sm oxide has totally reacted with other precursors to form the Bi-2212 phase and that Sm was well incorporated in the unit cell.

The percentage of the Bi-2212 phase in each sample was estimated using the following expression [30]:

$$Bi\text{–}2212\% = \frac{\sum I(2212)}{\sum I(2212 + 2201 + 2223)} \times 100 \quad (1)$$

where I (2212), I (2201), and I (2223) are the intensities of the XRD peaks identified for Bi-2212, Bi-2201, and Bi2223 phases, respectively.

The obtained values are listed in Table 2. They show that the Bi-2212 was the dominate phase and that Bi-2201 and Bi-2223 were impurity phases. We also estimated the texturing rate of the samples according to the (00l) plans by using the following relation [31]:

$$F_{00l}(\%) = (\sum I_{00l}/(\sum I_{2212} + \sum I_{SP})) \times 100 \quad (2)$$

where I_{00l}, I_{2212}, and I_{SP} are the intensities of the XRD peaks identified for (00l) planes, Bi-2212, and secondary phases, respectively. The obtained values are reported in the same table.

We note that the best texturing rate was found for the Sm10 sample. In order to get more information about the structure from the X-ray patterns, we performed the refinement using the Jana2006 program [24]. In this simulation, we have used the Le Bail method where the pseudo-Voigt function was chosen for the profile, the Simpson method for the asymmetry correction, and a polynomial for the background. In order to estimate the quality of our refinement, we have to check the agreement factors Rp, Rwp, and the goodness of fit (GOF) factor. We listed the values of these factors, the refined cell parameters (a, b, and $\boldsymbol{c}$), the cell volume, and modulation vector q in Table 2.The obtained values of Rp, Rwp, and GOF show the high quality of our refinement. The refinement confirms that Sm00 and Sm05 samples are crystallized in an orthorhombic structure with the Amaa space group (66), whereas the Sm10 transformed to a pseudo-tetragonal structure with the Fmmm space group (69) [32]. It revealed also the existence of the Bi-2201 and Bi-2223 as impurity phases. We note that the intensities of the peaks indexed by (006), (0080),

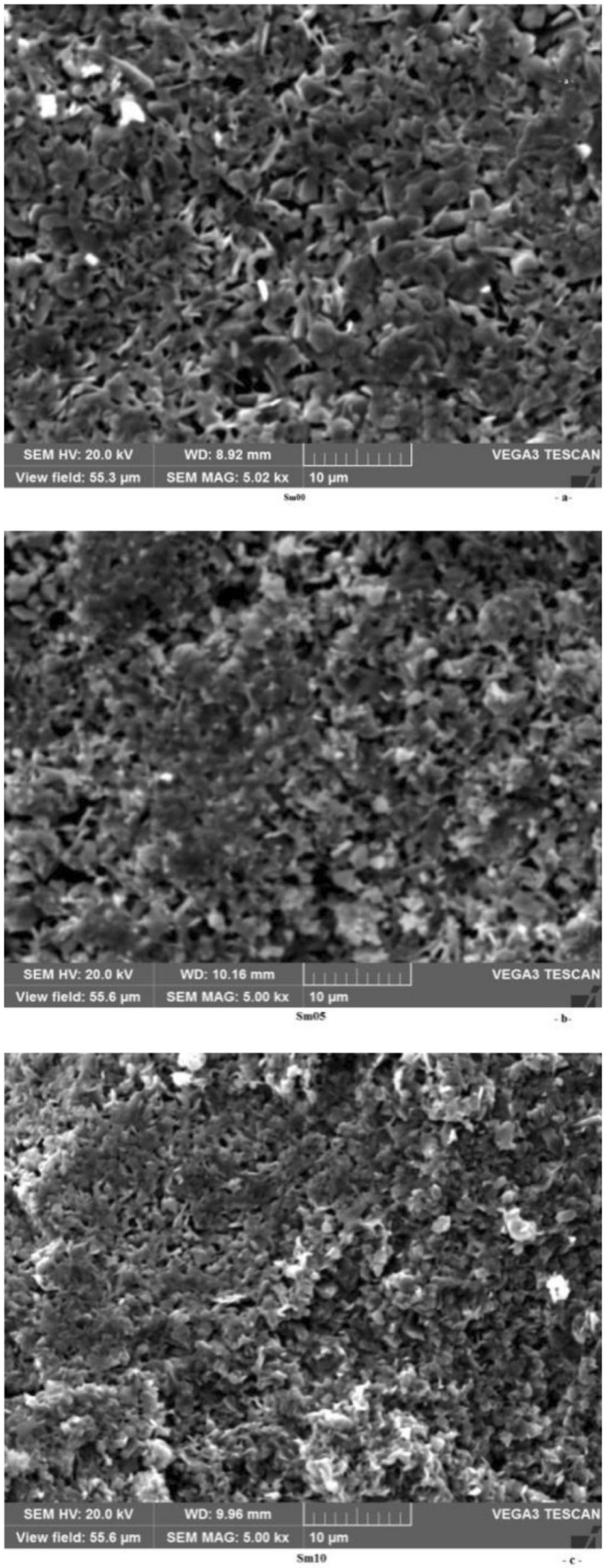

Fig. 5 SEM photographs of Sm00, Sm05, and Sm10 samples

(0010), (0012), and (0016) are intensified in the Sm10 sample. This implies the existence of preferred orientation along the c-axis of the crystallites [33]. From Table 2, we note a decrease of the parameter c. We believe that this result may be caused by two effects as follows: the difference of ionic radius between Bi (= 1.03 Å) and Sm (= 0.958 Å) [34] and the excess of oxygen incorporation into Bi-O layers causing a decrease of c parameter [35–37].

As it is known in the Bi-2212 phase, the omnipresent lattice distortions mainly appear in the Bi_2O_2 layers and cause a modulation in the structure. These distortions are caused by the mismatch of the different blocks of the cell due to the insertion of extra oxygen ions as reported by V. F. Shamraya et al. [38].The existence of the incommensurate modulation structure results in the appearance of satellite peaks in our XRD patterns. The satellite peaks were indexed with a 4-dimensional (hklm) space group Amaa(a00)000 with first-order satellites (m = ± 1), and the results of the indexation is presented in Table 3. Furthermore, the modulation vector q increases when samarium content increase. Such increase of the modulation period may be explained by the doping with the smaller ion radius element (Sm), which reduces the mismatch between the rock-salt layer and perovskite blocs [33].

The crystallite size D can be estimated from the Scherer's formula [39]:

$$D = \frac{K\lambda}{\beta cos\theta} \tag{3}$$

where K is a constant which is taken 0.9 in our case.

λ is the X-ray wavelength.
β is the full width of the peak (FWHM).
θ is the Bragg angle.

The estimated results are shown in Table 4. It is found that the crystallite size is in the nanometric scale and it ranges between 9.2 nm and 11.4 nm.

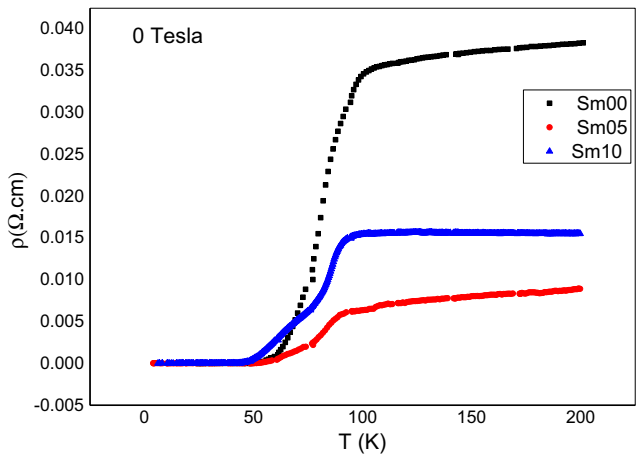

Fig. 6 Temperature dependence of resistivity of $Bi_{2-x}Sm_xSr_2CaCu_2O_{8+\delta}$ samples under zero magnetic field

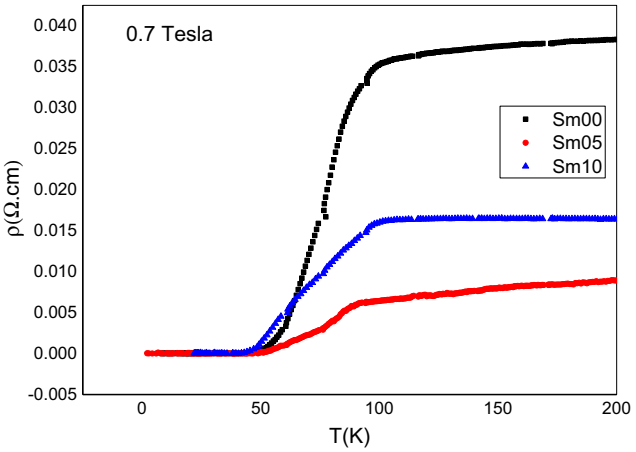

Fig. 7 Temperature dependence of resistivity of $Bi_{2-x}Sm_xSr_2CaCu_2O_{8+\delta}$ samples under 0.7 Tesla.

Figure 5 shows the morphology of our samples analyzed using a scanning electron microscopy with a magnification of ×5000. The SEM images show a granular porous character of the samples. It presents well-connected plate-shaped grains which are omnipresent in the Bi-based superconductor compounds [14]. With increasing Sm content, we observe a decrease of the grains and pores size, and hence, an increase of the densification.

Figures 6 and 7 present resistivity measurements of our samples. All our samples exhibit the superconductor state in the low temperature range. We present the T_C^{on}, T_C^{off}, T_C, and the transition width in Table 5. The undoped sample presents a single metal-superconductor transition. Its T_C^{on} and T_C^{off} are at 104.2 K and 56.9 K, respectively. These values are close to those found by Azhan et al. [40], who studied the same system of compounds prepared by the solid-state reaction technique. Our results show that the doping with Sm changed the electrical properties even it kept the transition between normal and superconductor states for all the samples. We note that the doping decreases the T_C^{off} and T_C. We observe that the transition width is more important in the case of the Sm05 sample than that of the Sm10 one. We believe that this may be related to the appearance of the Bi-2223 phase in the Sm05 sample.

Table 5 Onset and offset transition temperatures (Tc^{on}, Tc^{off}), transition width (ΔTc), and critical temperature (Tc) of $Bi_{2-x}Sm_xSr_2CaCu_2O_{8+\delta}$ samples

Sample	Sm00		Sm05		Sm10	
Applied magnetic field	0 T	0.7 T	0 T	0.7 T	0 T	0.7 T
Tc^{on}	104.2	103.7	108.5	108.1	100.4	99.7
Tc^{off}	56.9	48.3	51.9	49.1	44.5	39.4
ΔT	47.3	55.4	56.6	59	55.9	60.3
Tc	81	76.8	80.5	76.1	78.4	69.3

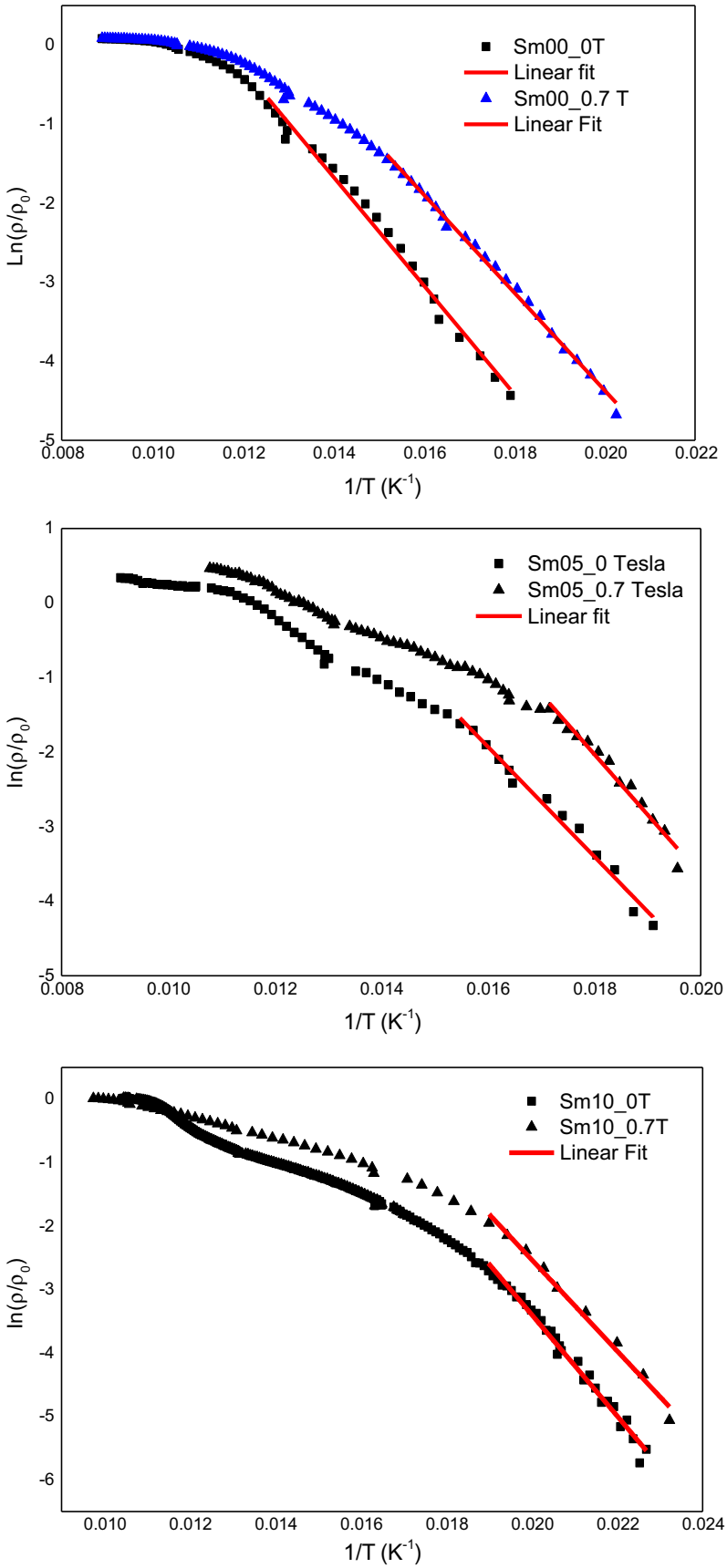

Fig. 8 Plot of $Ln(\rho/\rho_0)$ versus 1/T curves

Table 6 Residual resistivity (ρ_0) and activation energy (U_0) at different applied magnetic fields of $Bi_{2-x}Sm_xSr_2CaCu_2O_{8+\delta}$ samples

Sample	Sm00		Sm05		Sm10	
Applied magnetic field	0 T	0.7 T	0 T	0.7 T	0 T	0.7 T
ρ_0(Ω.cm)	0.033	0.033	0.005	0.004	0.015	0.016
U_0(meV)	59.3	53.4	63.6	52.9	68.9	52.04

Hence, we believe that doping with Sm decreases the values of the electrical properties and the appearance of this phase decreases them more. Moreover the Sm05 sample presents a second transition in the resistivity curves at around 108.5 K. This may be caused by the Bi-2223 phase, which its value is found to be around 110 K and 109 K by R. P. Aloysius et al. [41] and by Azhan et al. [40], respectively. We note here that the decrease of the critical temperature T_C in our case is in accordance with that found in previous works in the same phase or even in other phases [21].

Resistivity measurements under 0.7 Tesla as applied magnetic field, showed that the T_C^{on}'s remain almost unchanged, while T_C^{off}'s and T_C's decrease, in all samples,, which is in agreement with the work done by Özçelik et al. [42].

According to the thermally activated flux creep model [43], the experimental results in the tail part of the resistivity curves of the high Tc superconductor compounds have been found to follow the Arrhenius relation [44]. It is given bellow by Eq. 4.

$$\rho(\mathrm{T},\mathrm{H}) = \rho_0 \exp(-U_0(T,H)/K_B T) \quad (4)$$

where ρ_0 is the residual resistivity estimated by extrapolation of the curves in the normal state to 0 K, U_0 is the activation energy, and K_B is the Boltzmann constant.

In order to estimate the U_0(T,H) values, we have done a simulation using the Arrhenius relation and we have present the results in the Fig. 8 and Table 6. The slope of Arrhenius curves gives us the values of U_0. About ρ_0, we observe that the Sm05 sample shows the lowest value and the undoped sample has the highest value. This is explained in previous work of S. Boudjaoui et al. [44] by an increase of the disorder and inhomogeneity of grains distribution.

The obtained values of U_0 were in the range of 53.4 meV to 68.9 meV and the maximum value was obtained for the undoped sample under $H = 0$ T. Examining Table 6, we remark an increase of the U_0 values with Sm doping. The reason of this increase may be the decreasing of energy barriers with increasing of Sm content. However, with applying magnetic field, U_0 decreases, which is in agreement with previous works [45–47]. The decrease of U_0 may arise from the increase of the pinning centers' density, which is highly dependent on the applied magnetic field as reported by Zan et al. [48].

4 Conclusion

A series of Bi-2212 superconductor compounds were prepared by the Pechini method and investigated using various experimental techniques. The FTIR analysis showed that all the samples are free of organic elements after sintering. The XRD analysis revealed that the samples were crystallized in the Bi-2212 phase with orthorhombic structure (Amaa). The Bi-2201 phase appeared also as impurity phase in all the samples whereas Bi-2223 phase appeared only in the Sm05 sample. The cell parameters monotonically decreased with the Sm doping. This led to the transformation of the structure into a pseudo-tetragonal structure with Fmmm space group for the Sm10 sample. The modulation was incommensurate and increased with Sm content which is explained as a result of the mismatch decrease between the rock-salt layer and perovskite blocs. The crystallites' size was estimated and found to be in the nanometric scale. SEM analysis showed the granular and porous character of samples with well-connected plate-shaped grains. The electrical resistivity study showed that all the samples present the transition to the superconductor state. The Bi-2223 phase appeared in Sm05 caused a double transition in the tail part of resistivity curve. The critical temperature T_C decreased with the Sm doping, whereas the activation energy U_0 increased from 53.4 meV to 68.9 meV. A 0.7-T applied magnetic field led to a decrease of both T_C and U_0. The decrease of the U_0 is a result of the increasing of the pinning centers density.

Acknowledgments The authors would like to thank the Directorate General for Scientific Research and Technological Development—DGRSDT (PRFU Project N°. B00L02UN390120180003). The authors also acknowledge Dr. Michal Dusek, Senior Scientist at the Institute of Physics ASCRin Prague, Czech Republic, and Pr. Abderrezzak Amira, Professor at Mohammed Seddik Ben Yahia University, Jijel, Algeria for their advices.

References

1. Maeda, H., Tanaka, Y., Fukutomi, M., Asano, T.: A new high Oxidesuperconductor without a rare earth element. Jpn. J. Appl. Phys. **27**(2), L209 (1988)
2. Angurel, L.A., Díez, J.C., De la Fuente, G.F., Gimeno, F., Lera, F., López-Gascón, C., Martínez, E., Mora, M., Navarro, R., Sotelo, A., Andrés, N., Recuero, S., Arroyo, M.P.: Laser technologies applied to the fabrication and characterization of bulk bi-2212

superconducting materials for power applications. Phys. Status Solidi. **203**(11), 2931–2937 (2006)
3. Chen, M., Paul, W., Lakner, M., Donzel, L., Hoidis, M., Unternaehrer, P., Weder, R., Mendik, M.: 6.4 MVA resitive fault current limiter based on Bi-2212 superconductor. Physica C. **372–376**, 1657–1663 (2002)
4. Ahn, B.S.: Synthesis of BiSrCaCu(Ni)O ceramics from the gel precursors and the effect of Ni substitution. Bull. Kor. Chem. Soc. **23**, 1304 (2002)
5. Boussouf, N., Mosbah, M.F., Guerfi, T., Bouaicha, F., Chemekh, S., Amira, A.: Fe doping effect on structural properties of $Bi_{1.6}Pb_{0.4}Sr_2CaCu_{2-x}Fe_xO_{8+\delta}$. in: Proc. JMSM Conference. Phys. Procedia. **2**, 1153 (2008)
6. Zhang, Y., Yang, H., Li, M., Sun, B., Qi, Y.: Improvement of multiple oxide properties: effect of gel processes on the quality of $Bi_2Sr_2CaCu_2O_{8+\delta}$ superconducting powders. Cryst. Eng. Commun. **12**, 3046 (2010)
7. Prabhakaran, D., Subramanian, C.: Metal-insulator transition in the Pr substituted Bi-2212 bulk textured crystals. Physica C. **291**, 73 (1997)
8. Biju, A., Sarun, P.M., Aloysius, R.P., Syamaprasad, U.: Comparison of superconducting properties of Ce added (Bi, Pb)-2212 with other rare earth additions. J. Alloys Compd. **433**, 68 (2007)
9. Shabna, R., Sarun, P.M., Vinu, S., Biju, A., Guruswamy, P., Syamaprasad, U.: Metal-insulator transition and conduction mechanism in dysprosium doped $Bi_{1.7}Pb_{0.4}Sr_2Ca_{1.1}Cu_{2.1}O_{8+\delta}$ system. J. Appl. Phys. **104**, 013919 (2008)
10. Shabna, R., Sarun, P.M., Vinu, S., Syamaprasad, U.: Transport properties near the metal to insulator transition in samarium substituted (Bi,Pb)-2212 system. J. Appl. Phys. **105**, 113925 (2009)
11. Gao, Y.: Modulated structures of bismuth-based superconductors. Mater. Sci. Forum. **100-101**(273), (1992)
12. Biju, A., Kumar, R.G.A., Aloysius, R.P., Syamaprasad, U.: Structural and superconducting properties of $Bi_{1.7}Pb_{0.4}Sr_{2-x}Gd_xCa_{1.1}Cu_{2.1}O_y$ system. Physica C. **449**, 109 (2006)
13. Vinu, S., Sarun, P.M., Biju, A., Shabna, R., Guruswamy, P., Syamaprasad, U.: The effect of substitution of Eu on the critical current density and flux pinning properties of (Bi, Pb)-2212 superconductor. Supercond. Sci. Technol. **21**, 045001 (2008)
14. Biju, A., Sarun, P.M., Aloysius, R.P., Syamaprasad, U.: Superconductivity and flux pinning in Dy added (Bi, Pb)-2212 superconductor. Supercond. Sci. Technol. **19**, 1023 (2006)
15. Sedky, A., Al-Battat, W.: Effect of Y substitution at Ca site on structural and superconducting properties of Bi:2212 superconductor. Physica B. **410**, 227 (2013)
16. Özkurt, B.: Effects of Ni substitution in Bi-2212 superconductors. J. Supercond. Nov. Magn. **25**, 1775–1779 (2012)
17. Ulgen, A.T., Turgay, T., Terzioglu, C., Yildirim, G., Oz, M.: Role of Bi/Tm substitution in Bi-2212 system on crystal structure quality, pair wave function and polaronic states. J. Alloys Compd. **764**, 755–766 (2018)
18. Chandru, K., Selvanathan, G., Das, B.B.: Synthesis and characterization of samarium doped $SrBi_{2-x}O_4$ oxides. J. Appl. Chem. **10**, 38–43 (2017)
19. Uthayakumar, S., Srinivasan, E., Paul, D.P., Prabhakaran, D., Jayave, R., Subramanian, C., Ramasamy, P.: Texturing studies on Sm substituted Bi-2212 high T~ superconductor grown by floating zone technique. Physica C. **341-348**, 659–660 (2000)
20. Kishore, K.N., Muralidhar, M., Babu, V.H.: Effect of rare-earth Sm^{3+} substitution on the superconducting properties of the $Bi_{1.7}Pb_{0.3}Sr_2Ca_{2-x}Sm_xCu_30_y$ system. Physica C. **204**, 299–304 (1993)
21. Hamadneh, I., Halim, S.A., Leeb, C.K., Daud, W.M., Hassana, Z.A.: The influence of samarium doping in Bi1.6 (Pb0.4)Sr2-xSmxCa2Cu3Oy prepared by coprecipitation method. Solid State Sci Technol. **11**(1), 139–146 (2003)
22. Prabitha, V.G., Biju, A., Kumar, R.G.A., Sarun, P.M., Aloysius, R.P., Syamaprasad, U.: Effect of Sm addition on (Bi,Pb)-2212 superconductor. Physica C. **433**, 28–36 (2005)
23. Kim, H.S., Lee, G.J., Lee, J.Y., Lee, D.H., Kim, K.H.: Processing parameters and bond nature of SmxBi1-xSrCaCuO superconductor. Mater. Chem. Phys. **49**, 12–15 (1997)
24. Petricek, V., Dusek, M., Palatinus, L.: Crystallographic computing system JANA2006: general features. Z. Kristallogr. **229**(5), 345–352 (2014)
25. Arshad, M., Qureshi, A.H., Masud, K., Qasi, N.K.: Production of BSCCO bulk high Tc superconductors by sol-gel method and their characterization by FTIR and XRD techniques. J. Therm. Anal. Calorim. **89**, 595–600 (2007)
26. Zhang, Y., Yang, H., Li, M., Sun, B., Qi, Y.: Improvement of multiple oxide properties: effect of gel processes on the quality of $Bi_2Sr_2CaCu_2O_{8+d}$ superconducting powders. Cryst. Eng. Commun. **12**, 3046–3051 (2010)
27. Lee, K.S., Kim, K.D.: Efficient synthesis of primary amides from carboxylic acids using N,N'-Carbonyldiimidazole and ammonium acetate ionic liquid. Synth. Commun. **41**, 3497–3500 (2011)
28. Chen, T.M., Hiu, Y.H.: Pollymeric precursors for the preparation of $Bi_{1.5}Pb_{0.5}Sr_2Ca2Cu_3O_x$. J. Solid State Chem. **97**, 124–130 (1992)
29. Sama, C., Mosbah, M.-F., Attaf, S., Benbellat, N.: The effect of Ba doping on Sr site on structural and superconducting properties of Bi2212 phase. Physica B. **557**, 12–16 (2019)
30. Boussouf, N., Mosbah, M.-F., Bouaicha, F., Amira, A.: Effect of Magnesium on the Bi-based (2212) superconductors in: Proceeding of International Conference on Electronics, Dubai, 7–8 (2012) 318
31. Safran,S., Kiliç,A., Ozturk,O.: Effect of re-pelletization on structural, mechanical and superconducting properties of BSCCO superconductors. J. Mater. Sci. Mater. Electron. 28 (2)1799–1803 (2016)
32. Wesche, R.: Physical Properties of High-Temperature Superconductors, edition edn. John Wiley & Sons Ltd (2015)
33. Zhou, S., Wang, H., Wang, Y., Fei, Z., Sun, B., Qi, Y.: Study on incommensurate modulation structures in Ca-doped Bi-2201 System. J. Supercond. Nov. Magn. **27**, 383–388 (2014)
34. Shannon, R.D.: Revised effective ionic radii and systematic studies of interatomie distances in halides and chaleogenides. Acta Cryst. A. **32**, 751–767 (1976)
35. Terzioglu, C., Yilmazlar, M., Ozturk, O., Yanmaz, E.: Structural and physical properties of Sm-doped $Bi_{1.6}Pb_{0.4}Sr_2Ca_{2-x}Sm_xCu_3O_y$ superconductors. Physica C. **423**, 119–126 (2005)
36. Musolino, N., Bals, S., Van Tendeloo, G., Clayton, N., Walker, E., Flukiger, R.: Modulation-free phase in heavily Pb-doped (Bi, Pb)2212 crystals. Physica C. **399**, 1–7 (2003)
37. Mentré, O., Iorgulescu, M., Huvé, M., Kabbour, H., Renaut, N., Daviero-Minaud, S., Colisb, S., Roussel, P.: $BaCoO_{2.22}$: the most oxygen-deficient certified cubic perovskite. Dalton Trans. **44**(23), 10728–10737 (2015)
38. Shamray, V.F., Mikhailov, A.B., Mitin, A.V.: Crystal structure and superconductivity of Bi2223. Crystallogr. Rep. **54**(4), 584–590 (2009)
39. Chu, S., McHenry, M.E.: Growth and characterization of (Bi, Pb)$_2Sr_2Ca_2Cu_3O_x$ single crystals. J. Mater. Res. **13**(3), 589–595 (1998)
40. Azhan, H., Azura, C.M.N., Azman, K., Senawi, S.A., Syuhaida, I.N., Robaiah, M., Rosli, M.M.: Effect of Eu substitution in low density bi (Pb)-2223 high-temperature superconductors. Mater. Sci. Forum. **846**, 567–573 (2016)
41. Aloysius, R.P., Guruswamy, P., Syamaprasad, U.: Highly enhanced critical current density in Pr-added (Bi, Pb)-2212 superconductor. Supercond. Sci. Technol. **18**, L23–L28 (2005)
42. Özçelik, B., Kaya, C., Gündogmu, H., Sotelo, A., Madre, M.A.: Effect of Ce substitution on the magnetoresistivity and flux pinning

energy of the $Bi_2Sr_2Ca_{1-x}Ce_xCu_2O_{8+\delta}$. Superconduct. J. Low Temp. Phys. **174**, 136–147 (2014)
43. Erdem, M., Ozturk, O., Yucel, E., Altintas, S.P., Varilci, A., Terzioglu, C., Belenli, I.: Effect of Gd addition on the activation energies of Bi-2223 superconductor. Physica B. **406**, 705–709 (2011)
44. Boudjaoui, S., Amira, A., Mahamdioua, N., Altintas, S., Varilci, A., Terzioglu, C.: Substitution effect of Sr2+ by Ca2+ on structure and superconducting properties of $Bi_2Sr_{1.6}La_{0.4}CuO_{6+\delta}$ (Bi-2201) ceramics. Physica B. **531**, 58–63 (2017)
45. Kameli, P., Salamati, H., Abdolhosseini, I., Sohrabi, D.: Thermally activated flux creep in the $Bi_{1.66}Pb_{0.34}Sr_2Ca_{2-x}Mg_xCu_3O_y$ superconductors. Physica C. **468**, 137–141 (2008)
46. Pu, M.H., Cao, Z.S., Wang, Q.Y., Zhao, Y.: The influence of Cr-ions on the flux creep in Bi-2223/Ag tapes. Supercond. Sci. Technol. **19**, 462–465 (2006)
47. Palstra, T.T., Batlogg, B., Van Dover, R.B., Schneemeyer, L.F., Waszczak, J.V.: Dissipative flux motion in high-temperature superconductors. Phys. Rev. B. **41**, 6621–6632 (1990)
48. Zan, R., Ekicibil, A., Kiymaç, K.: Structural characterization and superconductivity in $Bi_{1.7}Pb_{0.3-x}Tb_xSr_2Ca_3Cu_4O_y$.The influence of Tb-doping. J. Optoelectron. Adv. Mater. **11**(3), 348–355 (2009)